Radioimmunotherapy of fibroblast activation protein positive tumors by rapidly internalizing antibodies

Fischer, Eliane ; Chaitanya, Krishna ; Wüest, Thomas ; Wadle, Andreas ; Scott, Andrew M ; van den Broek, Maries ; Schibli, Roger ; Bauer, Stefan ; Renner, Christoph

Abstract: PURPOSE: Fibroblast activation protein (FAP) is a serine protease that has emerged as a promising target for cancer therapy, either by direct abrogation of its proinvasive activity or by specific targeting of FAP-expressing cells with cytotoxic immunoconjugates. We aimed to select novel human-mouse cross-reactive antibodies and to test suitability for tumor therapy as radioimmunoconjugates in a preclinical model. EXPERIMENTAL DESIGN: Human Fab fragments that bind to human and murine FAP were selected from an antibody phage library. Two candidates (ESC11 and ESC14) were engineered into fully human IgG1 antibodies and further characterized. We investigated the intracellular trafficking of ESC11 and ESC14 in live cells by confocal microscopy and analyzed the biodistribution and therapeutic effects of anti-FAP antibodies labeled with the -emitting radionuclide (177)Lu in a melanoma xenograft nude mouse model. Results were compared with vF19, a humanized variant of an anti-FAP antibody that has been previously used in clinical trials. RESULTS: The two antibodies bound selectively to both human and mouse FAP, with affinities in the low nanomolar range. Binding to FAP-expressing melanoma cells resulted in rapid internalization of FAP-antibody complexes. (177)Lu-labeled ESC11 specifically accumulated in melanoma xenografts in vivo, with a higher tumor uptake than ESC14 and vF19. Radioimmunotherapy with 8 MBq (177)Lu-labeled anti-FAP antibodies delayed growth of established tumors, whereas (177)Lu-ESC11 extended mouse survival more pronounced than (177)Lu-ESC14 and (177)Lu-vF19. CONCLUSION: Our results show the potential of ESC11 and ESC14 as potent radioimmunoconjugates or antibody-drug conjugates for diagnostic and therapeutic use in patients with FAP-expressing tumors.

DOI: https://doi.org/10.1158/1078-0432.CCR-12-0644

Clinical Cancer Research

Radioimmunotherapy of Fibroblast Activation Protein positive tumors by rapidly internalizing antibodies

Eliane Fischer, Krishna Chaitanya, Thomas Wuest, et al.

Clin Cancer Res Published OnlineFirst September 19, 2012.

Radioimmunotherapy of Fibroblast Activation Protein positive tumors by rapidly internalizing antibodies

Eliane Fischer[‡,§,1], Krishna Chaitanya [‡,1] Thomas Wüest[‡], Andreas Wadle[‡], Andrew M. Scott[¶], Maries van den Broek[‡], Roger Schibli[§], Stefan Bauer[‡] and Christoph Renner[‡]

[‡] Division of Oncology, University Hospital Zürich, 8091 Zürich, Switzerland

[§]Center for Radiopharmaceutical Sciences, Paul Scherrer Institute, 5232 Villigen PSI, Switzerland

[¶]Ludwig Institute for Cancer Research, Melbourne, Australia

[1] These authors contributed equally

Running Title: Radioimmunotherapy by internalizing FAP-specific antibodies.

Keywords: Fibroblast activation protein; Melanoma; Antibodies; Radioimmunotherapy; SPECT/CT

Financial support: Ludwig Institute for Cancer Research/Atlantic Philanthropies (CR), Zürcher Krebsliga (TW, CR), Krebsforschung Schweiz (TW, EF, CR) and the University of Zürich (Forschungskredit to EF and SB).

Address correspondence to: Christoph Renner, Oncology Department, Universitätsspital Zürich, 8091 Zürich, Switzerland. E-mail: christoph.renner@usz.ch

Word count: 4915 (excl. references, abstract)

Number of Figures/Tables: 5/1

Translational relevance

Carcinoma-associated fibroblasts in epithelial cancers and tumor cells of melanoma or sarcoma origin express high levels of Fibroblast Activation Protein (FAP). In phase I/II clinical trials, first generation FAP-specific antibodies have demonstrated high tumor-selective expression of this antigen. The novel antibodies described in this study, ESC11 and ESC14, rapidly internalize into FAP-expressing cells and exhibit excellent *in vivo* targeting properties. Therefore, they are ideal scaffolds for the development of immunoconjugates with cytotoxic drugs or radiometals that are retained within the cells. Our preclinical studies using a melanoma model serve as a basis for the clinical development of the ESC11 and ESC14 antibodies for targeting FAP-expressing tumor cells or carcinoma-associated fibroblasts. Since both antibodies cross-react with rodent FAP, the relevance of preclinical studies is increased. Furthermore, translation to the clinic is facilitated because they are fully human antibodies.

Abstract

Purpose:

Fibroblast activation protein (FAP) is a serine protease that has emerged as a promising target for cancer therapy, either by direct abrogation of its pro-invasive activity or by specific targeting of FAP-expressing cells with cytotoxic immunoconjugates. We aimed to select novel human-mouse cross-reactive antibodies and to test suitability for tumor therapy as radioimmunoconjugates in a preclinical model.

Experimental design:

Human Fab fragments that bind to human and murine FAP were selected from an antibody phage library. Two candidates (ESC11 and ESC14) were engineered into fully human IgG1 antibodies and further characterized. We investigated the intracellular trafficking of ESC11 and ESC14 in live cells by confocal microscopy and analyzed the biodistribution and therapeutic effects of anti-FAP antibodies labeled with the β-emitting radionuclide ^{177}Lu in a melanoma xenograft nude mouse model. Results were compared with vF19, a humanized variant of an anti-FAP antibody that has been previously used in clinical trials.

Results:

The two antibodies bound selectively to both human and mouse FAP, with affinities in the low nanomolar range. Binding to FAP-expressing melanoma cells resulted in rapid internalization of FAP-antibody complexes. ^{177}Lu-labeled ESC11 specifically accumulated in melanoma xenografts *in vivo,* with a higher tumor uptake than ESC14 and vF19. Radioimmunotherapy with 8 MBq ^{177}Lu-labeled anti-FAP antibodies delayed growth of established tumors, whereby ^{177}Lu-ESC11 extended mouse survival more pronounced than ^{177}Lu-ESC14 and ^{177}Lu-vF19.

Conclusion:

Our results demonstrate the potential of ESC11 and ESC14 as potent radioimmunoconjugates or antibody-drug conjugates for diagnostic and therapeutic use in patients with FAP-expressing tumors.

Introduction

Fibroblast activation protein (FAP) has emerged as a key player in cancer physiology with multiple biological functions. Most prominently, FAP is highly expressed on carcinoma-associated fibroblasts, where it is thought to contribute to cancer initiation, progression, and metastasis (1-3). In addition, FAP is also present on some cancer cells, including bone and soft tissue sarcoma (4) and some melanoma (5). FAP is a type II transmembrane serine protease that gains its enzymatic activity upon homodimerization of two identical 97-kDa subunits (6, 7). The natural substrates of FAP are still not completely identified, but the protease is capable of cleaving N-terminal dipeptides from polypeptides with proline or alanine in the penultimate position (8) and also has collagenase activity (9-11). The dipeptidyl-peptidase activity of FAP is one of the mediators of tumor progression (12), extracellular matrix remodeling (13-18), and metastasis formation (10, 19), but recent studies strongly suggest additional effects of FAP in the absence of its enzymatic activity (20) by hitherto unclear mechanisms. Very recently, FAP-expressing stromal cells have been shown to suppress anti-tumor immunity (21), adding yet another aspect to the manifold contributions of FAP to tumor growth.

Because of this multifaceted influence on tumor physiology, its restricted expression pattern within diseased areas and correlation with poor clinical outcome in cancer patients (22, 23), FAP has emerged as a promising target for cancer therapy. A humanized version of mAb F19 (Sibrotuzumab), a first generation anti-FAP antibody, however, failed to demonstrate measurable therapeutic activity (24) in Phase I/II clinical trials despite excellent tumor stroma targeting properties (25). In addition, 8 out of 26 Sibrotuzumab treated patients developed human-anti-human antibodies (HAHA) with a change in pharmacokinetics and reduced tumor uptake in four of them. Therefore, further clinical development of Sibrotuzumab was halted.

Strategies to target cancer with modified FAP-specific antibodies have recently gained interest and new technologies for the conjugation of toxins or cytokines to FAP-specific antibodies have been established. For example, an antibody-maytansinoid conjugate (26) and antibody-TNF fusion proteins (27, 28) have shown promise at the preclinical stage and are pending clinical development.

Radioimmunotherapy, the targeted delivery of therapeutic radioisotopes to the tumor site by monoclonal antibodies, is an attractive strategy for cancer treatment. Notably, antigen expression is usually spatially heterogeneous within the tumor. With FAP being restricted to carcinoma-associated fibroblasts, the therapeutic efficacy can be augmented by the 'cross-fire' effect of β-emitting radionuclides on neighboring FAP-negative tumor cells. Clinical trials with ^{131}I-labeled Sibrotuzumab have been performed to investigate targeting properties and pharmacokinetics but were discontinued due to the above-mentioned issues associated with HAHA (25). While radioiodination with ^{131}I is relatively easy to perform, the radionuclide is readily released

from the tumor upon internalization into cells. In contrast, high doses of residualizing radioisotopes may accumulate at the tumor site with internalizing antibodies and lead to a persistent irradiation of the tumor tissue. The radiolanthanide ^{177}Lu has a comparable range of the β-particles in tissue as ^{131}I (2 mm and 3 mm, respectively). In contrast to the high-energy γ-photons of ^{131}I, which are a disadvantage from a radiation safety perspective, ^{177}Lu emits 208 keV γ-photons at much lower abundance (11%).

For preclinical evaluation of radioimmunoconjugates, human-mouse cross-reactive antibodies are preferentially used to detect possible accumulation in tissue expressing homologous FAP. This allows more accurate estimation of side effects that may arise from radioactive doses delivered to healthy organs. In addition, for targeting of the tumor stroma in preclinical models, cross-reactivity with the homologous antigen of the model species is a prerequisite.

In this report, we describe the successful selection of two human monoclonal antibodies, ESC11 and ESC14, from a phage-display library. In contrast with F19 (Sibrotuzumab), we found that these novel antibodies were rapidly internalized by FAP-positive cells. Using ESC11 and ESC14 labeled with the β-emitting radiolanthanide ^{177}Lu, we found that both antibodies specifically accumulated in xenografted FAP-positive human melanoma and delayed tumor growth *in vivo*.

Materials and Methods

Cells, Cell lines and Reagents

HEK293huFAP, HEK293muFAP and HEK293huCD26 were generated by cloning huFAP, CD26 or muFAP cDNA into the pEAK8 vector (Edge Biosystems) and stable transfection of HEK293 c-18 cells (ATCC CRL-10852) followed by monoclonalization by limited dilution. The cell lines were maintained in DMEM supplemented with 10 % fetal bovine serum (FBS), penicillin–streptomycin, and puromycin (3 µg/mL). HT1080 FAP^+, huFAP expressing HT1080 (ATCC CCL-121), were maintained in RPMI supplemented with 10 % FBS (Gibco, Invitrogen) and 200 µg/mL G418. Human melanoma cell lines SK-Mel-187 and SK-Mel-16 were kindly provided by Ludwig Institute for Cancer Research, New York, USA and maintained in RPMI 10 % FBS. Murine antibody F19 and human anti-A33 antibody were obtained from Ludwig Institute for Cancer Research, Melbourne, Australia. Humanized vF19 was generated by veneering of F19 and was supplied by the Ludwig Institute for Cancer Research, New York, USA.

Antibody selection by phage display

For selection of huFAP-muFAP specific antibodies, a non-immunized phage library expressing human antibody Fab fragments was used (29). Details of the selection procedure are outlined in the supplementary data.

Phage screening by ELISA

For screening of FAP-binding phage by ELISA, 96-well microtiter plates (MaxiSorp Nunc) were coated with cell extracts from HEK293 huFAP, HEK293 huCD26, HEK293 muFAP, or mock-transfected HEK293, blocked with 5 % milk powder in PBS, incubated with phage-containing supernatants for 1 hr at room temperature, and developed using an anti-M13-HRP conjugated antibody and TMB as substrate.

Expression of Fab fragments

Fab fragments were produced in *E. coli* TG-1 by induction with 1 mM IPTG for 4 hrs at 30 °C. Soluble Fab was released from the periplasmic fraction by incubation in PBS, pH 8 at 4 °C over night. Crude fractions were incubated with Talon™ resin (CLONTECH Laboratories) for 1 hr at 4 °C, washed with wash buffer (20 mM Tris, 100 mM NaCl, 0.1% Tween 20), eluted with 100 mM imidazole, and dialyzed against PBS at 4 °C over night.

Determination of kinetic rate constants and affinity by surface Plasmon resonance

Binding analysis of Fabs was performed on a BIAcore T100 instrument. Recombinant huFAP (R&D systems) was immobilized at low density on a CM5 sensor chip (Biacore AB) using amine coupling chemistry according to the manufacturer's instructions. ESC11 and ESC14 Fabs were injected in 10 mM HEPES, pH 7.4, 3.4 mM EDTA, 0.15 mM NaCl, and 0.005 % Tween 20 at a flow rate of 80 µL/min at 25 °C and concentrations ranging from 0.5-16 nM and 6.25-200 nM respectively. The sensor chip was regenerated between injections with 0.1 M sodium carbonate and rate constants were calculated using BIAevaluation data analysis program.

Cloning, expression, and purification of IgG1

The variable sequences of heavy and light chain were cloned via DraIII and RsrII sites, respectively, into a modified pEE12.4 vector (LONZA Biologics) encoding human constant IgG1 domains. Stable antibody producing cell lines were developed using NS0 cells and the glutamine synthetase selection system according to the manufacturer's instruction (LONZA Biologics). Human IgG were purified from the culture supernatant by binding to CaptureSelect Fab kappa Affinity Matrix (CaptureSelect; Netherlands) followed by elution with 0.1 mM Glycine pH 2.5 and dialysis against PBS at 4 °C over night.

Flow cytometry

Cells were harvested at 50 % confluence and stained with primary and secondary antibodies for 60 min and 30 min on ice, respectively. Each staining step was followed by 2 washing steps (1 mL PBS, 2 % FBS). Cells were fixed with 2 % PFA for 10 minutes on ice before performing flow cytometry. At least 10,000 cells were measured on a FACScan (BD) cytometer and analyzed using FlowJo software (Treestar). For determination of the apparent K_D, the mean fluorescence intensities of a serial dilution were plotted and a dose-response curve was fitted using the equation f=Bmax*abs(x)/($K_D$app+abs(x))+Ns*x with SigmaPlot software (Systat Software Inc.). Human primary antibodies were detected with FITC/DyLight488 conjugated goat-anti-human antibody, (Jackson Immunoresearch, cat. no. 109-485-003) (1:200 dilution) whereas murine antibodies were stained with anti-mouse DyLight 488 labeled antibody (Jackson Immunoresearch, cat. no.115-486-146) (1:200 dilution). Fab antibodies were detected with anti-myc tag antibody 9E10, followed by an anti-mouse immunoglobulin-PE conjugate, (Jackson Immunoresearch, cat. no. 115-165-003) (1:200 dilution) Quantification of cell-surface FAP in internalization experiments was performed after overnight incubation with human IgGs at 37°C. Cells were then stained with 10 µg/mL F19 followed by anti-mouse FITC-conjugated antibody and % FAP expression was

calculated relative to the mean fluorescence intensity of cells that have not been incubated with human IgG. In case of vF19, directly labeled ESC11 (DyLight™549) was used to detect cell-surface FAP.

Confocal microscopy

Cells were seeded on sterile 20 mm fibronectin-coated (Sigma F1141-1MG, at 10 10 µg/mL) coverslips (Deckglaser; Carolina Biological, Germany) in 12 well plates and grown to 20-30 % confluency. Cells were fixed with 2 % PFA on ice and permeabilized using Cytofix/Cytoperm solution (51-2090KZ; BD Biosciences). Primary antibodies were diluted in 1x Perm/Wash (51-2091KZ; BD Biosciences) at following dilutions: EEA1, 1:100 (2411; Cell Signaling Technologies), LAMP1, 1:1000 (ab24170; Abcam), F19, 1:100. All secondary antibodies were used at a 1:200 dilution and were obtained from Jackson Immunoresearch. Dynasore hydrate (D7693; Sigma) and EIPA (A3085; Sigma) were added 30 minutes before the experiment at a final concentration ranging from 0-100 µM and 0-10 µM respectively. Cells were fixed with DAPI anti-fade (Invitrogen). All images were acquired on Leica SP5 UV/Vis confocal microscope (Leica Microsystems) at the Center for Microscopy and Image Analysis (University of Zurich) using LAS AF software. Images were kept in 1024x1024 formats and acquired with a zoom factor of 4 at 700 Hz frequency with HCxAPO Lambda blue 63.0x oil UV objective lens at a numerical aperture of 1.40. Images were stored in Tagged Image File Format (TIFF) and further processed using Image J software.

For internalization experiments, cells were incubated with 30 µg/mL human IgGs for the indicated time. FAP was then detected with F19 and DyLight 549 anti-mouse antibody, (Jackson Immunoresearch, cat. no. 115-506-062) (1:200 dilution). After incubation with vF19, FAP was detected with directly conjugated ESC11-DyLight 549. Alternatively, internalization was directly induced and monitored by DyLight 549-conjugated human IgG1 (30 µg/mL).

Radiolabeling and quality control

Antibodies were labeled with ^{177}Lu using the chelator CHX-A''-DTPA (*N*-[(R)-2-Amino-3-(*p*-isothiocyanato-phenyl) propyl]-*trans*-(*S,S*)- cyclohexane-1,2-diamine-*N,N,N',N'',N''*-pentaacetic acid, B355; Macrocyclics). Conjugation was performed in borate buffer (0.07 M, pH 9.15) under metal-free conditions and using a 5-fold molar excess of CHX-A''-DTPA. The reaction mixture was incubated for 1 h at 37°C. For all antibodies, 0.5-1 moles CHX-A''-DTPA, were coupled per one mole IgG1, as determined by incubation of a fixed amount of conjugated antibody with increasing amounts of ^{111}In (Mallinckrodt). The conjugated antibody was separated from free CHX-A''-DTPA using a NAP-5 column equilibrated with ammonium acetate buffer

(0.25 M, pH 5.5). CHX-A''-DTPA-antibody conjugates were labeled with ^{177}Lu ([^{177}Lu]Cl_3 in 0.04 M HCl, ITG Isotope Technologies Garching-GmbH Garching; Germany) for 1 h at 37°C.

The reaction was quenched with 5 mM EDTA and after 5 min of incubation at 37 °C, the radiolabeled antibody was purified on a Superose™-12 FPLC column (Amersham Biosciences). Elution was carried out in PBS at a flow rate of 0.5 mL/min. Radiochemical purity was analyzed by FPLC. The immunoreactive fraction was determined on HT1080 FAP cells using the Lindmo method as previously described (30).

SPECT/CT

Post mortem SPECT scans (2 h, 180 s per view) were performed with a 4-head multiplexing multipinhole camera (NanoSPECT/CT; Bioscan Inc.) 72 h after injection of ^{177}Lu-CHX-A''-DTPA-IgG1 (8 MBq, 15 µg) into the tail vein of nude mice bearing an SK-MEL-187 tumor on the hind leg and an SK-MEL-16 tumor on the shoulder. SPECT data were reconstructed iteratively with HiSPECT software (Scivis GmBH). The fused SPECT and CT datasets were analyzed using InVivoScope post processing software (Bioscan Inc.).

Biodistribution of ^{177}Lu- labeled antibodies in nude mice bearing human FAP-positive SK-Mel-187 tumors

Female nu/nu mice (Charles River, Switzerland) were injected s.c. in the right hind leg with 5x10^6 SK-Mel-187 cells in RPMI: BD Matrigel™ (cat. 354248; BD Biosciences) = 1:1 in a final volume of 200 µL. Tumors were allowed to grow to ~200 mm^3 before animals were randomly divided into groups of six mice for biodistribution studies (four mice for time-dependent biodistribution of ^{177}Lu-ESC11). Four µg (3 MBq) of each radiolabeled antibody was injected intravenously in 100 µL PBS. Animals were sacrificed by cervical dislocation. Radioactivity for each organ was measured using a gamma counter. The experiments were approved by the local ethics committee for animal research.

Radioimmunotherapy with ^{177}Lu-labeled antibodies in nude mice bearing SK-Mel-187 tumors

Mice were injected subcutaneously with 5 x 10^6 FAP-positive SK-Mel-187 cells as described above and randomized into groups of 7-8 mice. 8 MBq radiolabeled antibody (100 µL in PBS, 15-17 µg) or 100 µL PBS was injected into the tail vein five days post tumor cell implantation. Tumor growth was measured every 2-3 days with a caliper and tumor volumes were calculated according to the formula: volume = length × $width^2$ × 0.52. Animals were sacrificed when tumor volumes exceeded 1000 mm^3. Additional mice were sacrificed 3 and 7 days after treatment with 8 MBq ^{177}Lu-ESC11 or ^{177}Lu-A33 and tumors were processed for immunohistochemistry.

Immunohistochemistry experiments

Whole sections (3 μm thickness) were cut from formalin-fixed, paraffin-embedded blocks. Tissues were mounted on glass slides and deparaffinized in xylene. Rehydration was carried out in decreasing concentrations of ethanol and stained with hematoxylin-eosin using standard histological techniques. Ki-67 immunohistochemistry was performed using the automated Bond Max platform (Leica Microsystems, Heerbrugg, Switzerland) with a rabbit monoclonal MIB-1 antibody (1:200; clone SP6, Neomarkers, LabVision). Heat-induced epitope retrieval pre-treatment was performed, using H2-Buffer (Leica Microsystems) and boiling at 95 °C for 30 minutes. Bound antibody was detected with a corresponding secondary antibody included in the Refine-DAB detection kit (Leica Microsystems).

Statistical analyses: Data were analyzed using Prism (version 5.01) software (Graph Pad, San Diego, CA). Survival times were analyzed by Kaplan-Meier analysis, followed by the log-rank test. To correct for multiple comparisons of survival times, the Bonferroni corrected threshold was applied to determine significance.

Results

Selection and characterization of mouse-human FAP cross-reactive antibody Fab fragments

Monoclonal antibody Fab-fragments were selected from a large human Fab antibody library by phage display. The first four panning rounds were performed on human FAP (huFAP) (Supplementary Figure S1). Enrichment for Fab-fragments that cross-reacted with mouse FAP (muFAP) was performed in the fifth panning round (Supplementary Table 1). Screening of 300 selected clones by ELISA followed by PCR fingerprinting and sequencing of FAP-specific binders (data not shown) led to the identification of Fabs ESC11 and ESC14. By ELISA, both Fab fragments specifically bound to huFAP and muFAP and did not cross-react with the homologous protein CD26 (Figure 1A). Furthermore, Fab ESC11 and ESC14 bound to native FAP on the cell membrane of muFAP or huFAP expressing cells (Figure 1B). The binding affinity to recombinant huFAP was determined by surface plasmon resonance measurement using chips coated with a low-density of huFAP. K_D values of 10 ± 5 nM and 210 ± 35 nM were calculated for Fabs ESC11 and ESC14, respectively (Figure 1C). Similar affinities were determined by flow cytometry with calculated $K_D$apps on huFAP expressing cells of 4.7 ± 1.6 nM for ESC11 and 200 nM for ESC14, respectively (Table 1). On muFAP expressing cells, $K_D$apps were 51 ± 11 nM for ESC11 and 251 ± 42 nM for ESC14 (Table 1).

Preparation and characterization of IgG1 antibodies ESC11 and ESC14

The variable heavy chain (HC) and light chain (LC) domains of ESC11 and ESC14 were cloned and expressed as fully human IgG1. IgG1 was purified by affinity chromatography from cell culture supernatant to >95 % purity (Supplementary Figure S2). As expected, the binding affinity of bivalent IgG1 for huFAP was higher than that of monovalent Fab due to avidity effects with apparent K_D values around 1.1 nM on huFAP for both ESC11 and ESC14 IgGs (Table 1). These binding affinities are about 4-fold higher than for vF19 IgG. Interestingly, affinity constants of both ESC11 and ESC14 for muFAP were similar (around 2 nM) after conversion to IgG1.

Epitope mapping by competitive binding assay

To investigate whether ESC11 and ESC14 recognize different epitopes of FAP, we used ESC11 to compete with ESC14 or F19 for binding to native surface human FAP and vice versa followed by flow cytometry. Binding of ESC11 Fab could be blocked by ESC14 IgG and vice versa, while F19 (28), did not compete with either of the ESC antibodies for FAP binding (Supplementary Figure S3). These results suggest

that antibodies ESC11 and ESC14 recognize the same epitope or overlapping /spatially close epitopes that are different from the epitope recognized by the F19 antibody.

ESC11 and ESC14 IgG1 induce down-modulation and internalization of surface FAP

Incubation of SK-MEL-187, a FAP-expressing melanoma cell line, with F19, ESC11 or ESC14 on ice resulted in detectable surface staining. However, incubation at 37 °C for three hours with ESC11 or ESC14, but not with F19, induced internalization of FAP-antibody complexes (Figure 2A and 2B). This was not observed with monovalent Fabs indicating that cross-linking of FAP molecules by bivalent IgG1 was essential (data not shown). Internalization of surface FAP occurred very rapidly. Already after 20 min at 37 °C, an almost complete co-localization of internalized antibody with early endosomes could be observed, while after 40 min co-localization with LAMP-1, a marker for late endosomes and lysosomes (Figure 2C) was seen. We next tested pharmacological inhibitors of both dynamin-dependent endocytosis (dynasore) and macropinocytosis (EIPA) to investigate the mechanism of endocytosis. Dynasore inhibited antibody-mediated FAP internalization (Supplementary Figure S4A) while EIPA had no effect (Supplementary Figure S4B) demonstrating that endocytosis is mediated by a dynamin-dependent mechanism.

After overnight incubation with ESC11 and ESC14 antibodies, only very little FAP was detectable by flow cytometry on the surface of SK-MEL-187 cells. In contrast, still around 80 % of cell-surface FAP could be detected after prolonged incubation with vF19 (Figure 3A). We next investigated the time- and concentration-dependency of the observed FAP-down-modulation for ESC11. Overnight internalization was concentration dependent and the half-maximal effective concentration (EC50) was 3.3 ±0.5 nM (Figure 3B). At this concentration, most of the FAP epitopes are occupied by ESC11 antibody, which presumably results in rafting of FAP molecules and concomitant internalization. To assess time-dependency, we then chose a concentration of 200 nM at which FAP down-modulation is expected to be >90%. FAP was rapidly internalized, and the majority of FAP molecules disappeared from the cell surface within one hour (Figure 3C). When excess antibody was removed after overnight incubation, full FAP expression was restored not before three days after antibody removal (Figure 3D). In contrast, FAP expression remained low when ESC11 was present over the entire observation period.

mAb ESC11 specifically accumulates in human melanoma xenografts *in vivo*

ESC11, ESC14, vF19 and A33 were conjugated with CHX-A''-DTPA and subsequently labeled with ^{177}Lu. Radiochemical purity was > 95 % by FPLC for all four antibodies, and the specific activities were 0.4-

0.45 MBq/µg. Immunoreactivity of the radiolabeled antibodies was between 50 and 70% as determined by Lindmo analysis. All three ^{177}Lu-labeled FAP-binding antibodies bound specifically to SK-MEL-187 cells and could be displaced with increasing amounts of unlabeled antibody, while only a low amount of non-specific binding could be observed on the FAP-negative SK-MEL-16 cells (data not shown). Accordingly, SPECT/CT imaging 72 hrs post injection showed high and specific uptake of ^{177}Lu-ESC11 in the SK-MEL-187 tumor (Figure 4A), but low uptake in a SK-MEL-16 xenograft. Specific uptake was also observed with ^{177}Lu-vF19 in the FAP-expressing tumor (Figure 4B), while the control antibody ^{177}Lu-A33 did not accumulate in either tumor (Figure 4C).

Biodistribution data showed very high uptake of the three antibodies in FAP-expressing tumors 72 hrs post injection, and low activity in non-targeted organs (Figure 4D). Notably, ^{177}Lu-vF19 and, to a lesser extent, ^{177}Lu-ESC14 showed higher accumulation in the spleen than ^{177}Lu-ESC11, and cleared faster from the blood, which resulted in a reduced uptake in the tumors.

The *in vivo* biodistribution of ^{177}Lu- ESC11 was further studied over time in nude mice bearing human SK-MEL-187 tumor xenografts. We found a high (36 % of the injected dose per gram of tumor tissue after 48 h) and prolonged up-take of ^{177}Lu- ESC11, whereas its presence in blood and other organs was relatively low (Figure 4E). Radioactivity in melanoma xenografts accumulated until approximately 48 h post injection. After this time point, uptake values in the tumors remained high, but also became more variable in the individual mice, most likely due to the inhomogeneous tumor growth observed for this tumor model.

Radioimmunotherapy of established melanoma xenografts with ^{177}Lu-labeled FAP-specific antibodies

Next, we investigated the therapeutic efficacy of a single dose of the ^{177}Lu-radioimmunoconjugates *in vivo*. We estimated a dose of 8 MBq to be therapeutically active (31) and this dose has been shown to be well below the maximum tolerated dose in this mouse strain with other antibodies displaying similar biodistribution properties. Eight MBq (15 µg) ^{177}Lu-labeled antibodies were injected intravenously into nude mice bearing established subcutaneous human melanoma tumors (appr. 150 mm^3), 5 days post tumor implantation. Tumor growth was delayed with all three anti-FAP antibodies, and ^{177}Lu-ESC11 exhibited the most pronounced growth delay (Figure 5A). Analysis of survival curves (Figure 5B) showed an increase of median survival from 18 days (^{177}Lu-A33) to 32 days (^{177}Lu-vF19), 43 days (^{177}Lu-ESC14) and >43 days (^{177}Lu-ESC11) post tumor implantation. Additional mice were sacrificed on day 0, 3 and 7 after injection of radioimmunoconjugates and tumor specimens were processed for immunohistochemistry. We found a substantial reduction of proliferating (Ki67$^+$) tumor cells in samples taken after 3 and 7 days after injection of ^{177}Lu- ESC11 but not of the control

conjugate (Figure 5C). In addition, we observed increasing cell-free areas over time in the tumors treated with radiolabeled ESC11 (Figure 5D).

Discussion

We here describe the selection of novel human-mouse FAP-specific antibodies which down-modulate FAP expression from the surface of tumor cells, thus converting them into FAP-negative cells. Therapeutic strategies that aim at the complete down-modulation of FAP expression from the cellular surface might be promising approaches *per se*, since FAP is involved in cell invasion and metastatic processes of many cancers. Thus, antibody-induced internalization of cell surface-expressed FAP could provide major therapeutic impact by disturbing the various interactions on the cellular membrane, for example the formation of functional invadopodia.

But more importantly, the rapid internalization renders them perfect carrier proteins for the targeted destruction of FAP positive carcinoma-associated fibroblasts or tumor cells. These approaches have the potential to be much more efficient than therapy with naked antibodies (32). While internalization of the antibody is not a prerequisite for successful radioimmunotherapy with a β-particle emitting radionuclide like ^{177}Lu, it becomes a clear advantage when using α-particle or Auger-electron emitting radionuclides instead. In these cases, the vicinity of the internalized radionuclide to the cellular nucleus augments the therapeutic efficacy by introducing more damage to the radiation-sensitive DNA. Antibody-drug conjugates are a second example for which internalization is an important feature, especially when the drug is coupled to the antibody by an acid-labile linker, releasing the cytotoxic drug in the acidic lysosomes.

We have chosen human melanoma as a model system because the interaction between tumor cells and carcinoma-associated fibroblasts seems to be crucial for tumor growth and the development of drugs resistance (33). As shown by Flach and colleagues, melanoma cells stimulate the recruitment of fibroblasts and activate them by a so far unknown mechanism. In turn, these activated fibroblasts contribute to melanoma progression by providing both structural and chemical support (33). Incomplete abolishment of tumor cells by a short duration of kinase inhibitor therapy led to a transient reduction of tumor cells that was counteracted by an accelerated re-growth of tumor cells supported by the large fibroblast population that remained post-treatment. According to their model, the sole elimination of tumor cells is insufficient to provide tumor control and only a combined approach targeting tumor cells and carcinoma-associated fibroblasts simultaneously will lead to long lasting remissions.

FAP is not ubiquitously expressed in human melanoma at all stages of disease but is transiently present during the development of malignancy, and is routinely confined to the stromal fibroblasts in metastatic

melanoma (34). However, high expression levels of FAP have been shown to correlate with a pronounced invasive phenotype *in vitro* (35) and have recently been postulated to contribute to transmigration of melanoma cells through the blood-brain barrier (36).

In this study, we compared the *in vivo* targeting properties of the human-mouse cross-reactive antibodies ESC11 and ESC14 to vF19. In a model with relatively high antigen expression on the tumor cells, high accumulation of up to 50 % of the injected dose per gram tumor was observed. The only previously reported biodistribution experiment with a FAP-targeting antibody in mice was a study with human skin-grafted SCID mice bearing breast cancer tumors and a ^{131}I-labeled antibody (37). There, much lower accumulation in the tumor and less favorable tumor-to-organ ratios were achieved, presumably as a result of the tumor model and the choice of the metabolically less stable radiolabel. In phase I clinical trials, ^{131}I-labeled mAb F19 and its CDR-grafted humanized variant have been used to study pharmacokinetics, biodistribution and imaging characteristics in patients with metastatic cancer (25, 38, 39). FAP was efficiently targeted by mAb F19 in all patients and its expression was confined to the stroma of metastatic lesions. Given the high expression of FAP in human cancers and the restriction to diseased tissue, FAP is a promising target both for imaging and radioimmunotherapy.

In particular, targeting stromal fibroblasts instead of tumor cells has several appealing advantages: The highly vascularized stroma is thought to be reached more efficiently by bulky molecules such as monoclonal antibodies. Antigen expression is considered to be more stable in carcinoma-associated fibroblasts than in highly proliferating cancer cells.

Further, in many human epithelial cancers, stromal fibroblasts are highly abundant, and the cross-fire effect of low energy beta-emitting radionuclides (penetration of 2 mm in tissue) additionally contributes to the eradication of antigen-negative tumor cells and to a homogenous deposition of the dose within the tumor tissue. A recent study demonstrated that antitumor immunity is suppressed by FAP positive stromal cells (21), which adds to the importance of FAP in tumor physiology. Thus, human-mouse crossreactive FAP-specific antibodies are excellent tools to address this phenomenon *in vivo* by specific targeting of FAP-positive stromal fibroblasts and may help to unravel the mechanisms involved in local immunosuppression and tumor promotion.

In conclusion, we have developed novel fully human antibodies with excellent *in vivo* targeting properties. Due to their efficient internalization and targeting to the lysosomes, they are promising scaffolds for future development of antibody-drug conjugates or radioimmunotherapeutics.

Acknowledgements

We thank Susan Cohrs and Sascha Kleber for excellent technical assistance.

Grant support

Ludwig Institute for Cancer Research/Atlantic Philanthropies (CR), Zürcher Krebsliga (TW, CR),

Krebsforschung Schweiz (TW, EF, CR) and the University of Zürich (Forschungskredit to EF and SB).

References

1. Bhowmick NA, Neilson EG, Moses HL. Stromal fibroblasts in cancer initiation and progression. Nature. 2004;432:332-7.
2. Hwang RF, Moore T, Arumugam T, Ramachandran V, Amos KD, Rivera A, et al. Cancer-associated stromal fibroblasts promote pancreatic tumor progression. Cancer Research. 2008;68:918-26.
3. Karnoub AE, Dash AB, Vo AP, Sullivan A, Brooks MW, Bell GW, et al. Mesenchymal stem cells within tumour stroma promote breast cancer metastasis. Nature. 2007;449:557-63.
4. Dohi O, Ohtani H, Hatori M, Sato E, Hosaka M, Nagura H, et al. Histogenesis-specific expression of fibroblast activation protein and dipeptidylpeptidase-IV in human bone and soft tissue tumours. Histopathology. 2009;55:432-40.
5. Huber MA, Kraut N, Park JE, Schubert RD, Rettig WJ, Peter RU, et al. Fibroblast activation protein: differential expression and serine protease activity in reactive stromal fibroblasts of melanocytic skin tumors. J Invest Dermatol. 2003;120:182-8.
6. Aoyama A, Chen WT. A 170-kDa membrane-bound protease is associated with the expression of invasiveness by human malignant melanoma cells. Proceedings of the National Academy of Sciences of the United States of America. 1990;87:8296-300.
7. Kelly T. Evaluation of seprase activity. Clinical & Experimental Metastasis. 1999;17:57-62.
8. Garin-Chesa P, Old LJ, Rettig WJ. Cell surface glycoprotein of reactive stromal fibroblasts as a potential antibody target in human epithelial cancers. Proceedings of the National Academy of Sciences of the United States of America. 1990;87:7235-9.
9. Aggarwal S, Brennen WN, Kole TP, Schneider E, Topaloglu O, Yates M, et al. Fibroblast activation protein peptide substrates identified from human collagen I derived gelatin cleavage sites. Biochemistry (Mosc). 2008;47:1076-86.
10. Park JE, Lenter MC, Zimmermann RN, Garin-Chesa P, Old LJ, Rettig WJ. Fibroblast activation protein, a dual specificity serine protease expressed in reactive human tumor stromal fibroblasts. Journal of Biological Chemistry. 1999;274:36505-12.
11. Christiansen VJ, Jackson KW, Lee KN, McKee PA. Effect of fibroblast activation protein and alpha2-antiplasmin cleaving enzyme on collagen types I, III, and IV. Archives of biochemistry and biophysics. 2007;457:177-86.
12. Cheng JD, Valianou M, Canutescu AA, Jaffe EK, Lee HO, Wang H, et al. Abrogation of fibroblast activation protein enzymatic activity attenuates tumor growth. Molecular Cancer Therapeutics. 2005;4:351-60.
13. Ghersi G, Dong H, Goldstein LA, Yeh Y, Hakkinen L, Larjava HS, et al. Regulation of fibroblast migration on collagenous matrix by a cell surface peptidase complex. Journal of Biological Chemistry. 2002;277:29231-41.
14. Wang XM, Yu DM, McCaughan GW, Gorrell MD. Fibroblast activation protein increases apoptosis, cell adhesion, and migration by the LX-2 human stellate cell line. Hepatology. 2005;42:935-45.
15. Kennedy A, Dong H, Chen D, Chen WT. Elevation of seprase expression and promotion of an invasive phenotype by collagenous matrices in ovarian tumor cells. International Journal of Cancer. 2009;124:27-35.
16. Mueller SC, Ghersi G, Akiyama SK, Sang QX, Howard L, Pineiro-Sanchez M, et al. A novel protease-docking function of integrin at invadopodia. Journal of Biological Chemistry. 1999;274:24947-52.

17. Wolf BB, Quan C, Tran T, Wiesmann C, Sutherlin D. On the edge of validation--cancer protease fibroblast activation protein. Mini Reviews in Medicinal Chemistry. 2008;8:719-27.
18. Lee HO, Mullins SR, Franco-Barraza J, Valianou M, Cukierman E, Cheng JD. FAP-overexpressing fibroblasts produce an extracellular matrix that enhances invasive velocity and directionality of pancreatic cancer cells. BMC Cancer. 2011;11:245.
19. Niedermeyer J, Enenkel B, Park JE, Lenter M, Rettig WJ, Damm K, et al. Mouse fibroblast-activation protein--conserved Fap gene organization and biochemical function as a serine protease. European Journal of Biochemistry. 1998;254:650-4.
20. Huang Y, Simms AE, Mazur A, Wang S, Leon NR, Jones B, et al. Fibroblast activation protein-alpha promotes tumor growth and invasion of breast cancer cells through non-enzymatic functions. Clin Exp Metastasis. 2011;28:567-79.
21. Kraman M, Bambrough PJ, Arnold JN, Roberts EW, Magiera L, Jones JO, et al. Suppression of antitumor immunity by stromal cells expressing fibroblast activation protein-alpha. Science. 2010;330:827-30.
22. Cohen SJ, Alpaugh RK, Palazzo I, Meropol NJ, Rogatko A, Xu Z, et al. Fibroblast activation protein and its relationship to clinical outcome in pancreatic adenocarcinoma. Pancreas. 2008;37:154-8.
23. Henry LR, Lee HO, Lee JS, Klein-Szanto A, Watts P, Ross EA, et al. Clinical implications of fibroblast activation protein in patients with colon cancer. Clinical Cancer Research. 2007;13:1736-41.
24. Hofheinz RD, al-Batran SE, Hartmann F, Hartung G, Jager D, Renner C, et al. Stromal antigen targeting by a humanised monoclonal antibody: an early phase II trial of sibrotuzumab in patients with metastatic colorectal cancer. Onkologie. 2003;26:44-8.
25. Scott AM, Wiseman G, Welt S, Adjei A, Lee FT, Hopkins W, et al. A Phase I dose-escalation study of sibrotuzumab in patients with advanced or metastatic fibroblast activation protein-positive cancer. Clin Cancer Res. 2003;9:1639-47.
26. Ostermann E, Garin-Chesa P, Heider KH, Kalat M, Lamche H, Puri C, et al. Effective immunoconjugate therapy in cancer models targeting a serine protease of tumor fibroblasts. Clinical Cancer Research. 2008;14:4584-92.
27. Bauer S, Adrian N, Williamson B, Panousis C, Fadle N, Smerd J, et al. Targeted bioactivity of membrane-anchored TNF by an antibody-derived TNF fusion protein. Journal of Immunology. 2004;172:3930-9.
28. Bauer S, Adrian N, Fischer E, Kleber S, Stenner F, Wadle A, et al. Structure-activity profiles of Ab-derived TNF fusion proteins. Journal of Immunology. 2006;177:2423-30.
29. de Haard HJ, van Neer N, Reurs A, Hufton SE, Roovers RC, Henderikx P, et al. A large non-immunized human Fab fragment phage library that permits rapid isolation and kinetic analysis of high affinity antibodies. Journal of Biological Chemistry. 1999;274:18218-30.
30. Knogler K, Grünberg J, Novak-Hofer I, Zimmermann K, Schubiger PA. Evaluation of 177Lu-DOTA-labeled aglycosylated monoclonal anti-L1-CAM antibody chCE7: influence of the number of chelators on the in vitro and in vivo properties. Nucl Med Biol. 2006;33:883-9.
31. Fischer E, Grunberg J, Cohrs S, Hohn A, Waldner-Knogler K, Jeger S, et al. L1-CAM-targeted antibody therapy and (177) Lu-Radioimmunotherapy of disseminated ovarian cancer. Int J Cancer. 2011.
32. Casi G, Neri D. Antibody-drug conjugates: Basic concepts, examples and future perspectives. Journal of controlled release : official journal of the Controlled Release Society. 2012;161:422-8.
33. Flach EH, Rebecca VW, Herlyn M, Smalley KS, Anderson AR. Fibroblasts contribute to melanoma tumor growth and drug resistance. Mol Pharm. 2011;8:2039-49.

34. Rettig WJ, Garin-Chesa P, Healey JH, Su SL, Ozer HL, Schwab M, et al. Regulation and heteromeric structure of the fibroblast activation protein in normal and transformed cells of mesenchymal and neuroectodermal origin. Cancer Res. 1993;53:3327-35.
35. Monsky WL, Lin CY, Aoyama A, Kelly T, Akiyama SK, Mueller SC, et al. A potential marker protease of invasiveness, seprase, is localized on invadopodia of human malignant melanoma cells. Cancer Res. 1994;54:5702-10.
36. Fazakas C, Wilhelm I, Nagyoszi P, Farkas AE, Hasko J, Molnar J, et al. Transmigration of melanoma cells through the blood-brain barrier: role of endothelial tight junctions and melanoma-released serine proteases. PloS one. 2011;6:e20758.
37. Tahtis K, Lee FT, Wheatley JM, Garin-Chesa P, Park JE, Smyth FE, et al. Expression and targeting of human fibroblast activation protein in a human skin/severe combined immunodeficient mouse breast cancer xenograft model. Mol Cancer Ther. 2003;2:729-37.
38. Welt S, Divgi CR, Scott AM, Garin-Chesa P, Finn RD, Graham M, et al. Antibody targeting in metastatic colon cancer: a phase I study of monoclonal antibody F19 against a cell-surface protein of reactive tumor stromal fibroblasts. J Clin Oncol. 1994;12:1193-203.
39. Tanswell P, Garin-Chesa P, Rettig WJ, Welt S, Divgi CR, Casper ES, et al. Population pharmacokinetics of antifibroblast activation protein monoclonal antibody F19 in cancer patients. Br J Clin Pharmacol. 2001;51:177-80.

Table 1: Apparent affinities of anti-FAP antibodies on huFAP and muFAP

Figure 1. Specificity and affinity of Fabs ESC11 and ESC14. (A) Binding of Fabs ESC11 and ESC14 (100 nM) in ELISA to plate immobilized membrane fractions of HT1080 FAP^+ (black bars), HT1080 (white bars), HEK293 $huCD26^+$ (striped bars), HEK293 $muFAP^+$ (grey bars), HEK293 mock transfected line (hatched bars). (B) FACS analysis of Fab ESC11 (black line), ESC14 (grey line), and a non-binding control Fab (filled) on HT1080 FAP^+ cells (left) and 293 $muFAP^+$ cells (right). (C) Affinity of Fabs ESC11 (left) and ESC14 (right) was determined by surface plasmon resonance. Purified Fabs were injected at the indicated concentrations on a rhuFAP-coated CM5 sensor chip.

Figure 2. Antibody-induced internalization of FAP. A. Representative confocal microscopy images of SK-Mel-187 cells incubated with Anti-FAP antibodies for 3 hours. FAP staining is shown in red. **B.** Spatial localization of DyLight 549-labeled anti-FAP antibodies on SK-MEL-187 cells after 3 hours incubation at 37°C. **C.** Colocalization of FAP and endosomes: SK-Mel-187 cells were incubated with ESC11 IgG1 and localization of FAP (DyLight 549-F19; red) was followed by staining early endosomes (EEA1; green) and late endosomes/early lysosomes (LAMP-1; green). The merge of the three images is shown in the right panel. Yellow indicates colocalization of FAP with endosomal markers.

Figure 3. Comparative FAP down-modulation capabilities of anti-FAP antibodies *in vitro*: **A.** SK-Mel-187 cells were incubated overnight with the indicated antibodies. **B.** FAP down-modulation pattern after incubation with ESC11 IgG1 on FAP-positive (SK-Mel-187; solid circles with fitted sigmoid dose-response curve (dashed line)) and FAP-negative (SK-Mel-16; solid squares) human melanoma cell lines and with isotype control antibody, A33 (on SK-Mel-187; solid triangles). **C.** Time-dependent FAP down-modulation by ESC11 IgG1 on SK-Mel-187 cells (solid circles) and SK-Mel-16 cells (solid squares) and isotype control antibody (solid triangles) on SK-Mel-187 cells at t=0 (initial) and t=5 (final) time points. **D.** Time kinetics of FAP reappearance on SK-Mel-187 cell surface. Solid squares: ESC11 added at t=0 and removed at t=14 hours; Solid triangles: ESC11 added at t=0; Solid circles: no antibody added.

All results are presented as percent values normalized to receptor positive cells in the absence of any antibody. Error bars: SD (n=3).

Figure 4. Biodistribution of ^{177}Lu-labeled FAP-specific antibodies. *Post mortem* SPECT/CT images showing biodistribution of **A** ^{177}Lu-CHX-A´´-DTPA-ESC11, **B** ^{177}Lu-CHX-A´´-DTPA-vF19 and **C** ^{177}Lu-CHX-A´´-DTPA-A33 in nude mice 72 h post injection. **D.** Biodistribution of ^{177}Lu-labeled antibodies in mice bearing SK-Mel-187 xenografts 72 hrs post injection. ^{177}Lu-ESC11 (black bars), ^{177}Lu-ESC14 (striped bars) ^{177}Lu-vF19 (grey bars) and ^{177}Lu-A33 (white bars). **E.** Time-dependent biodistribution of ^{177}Lu-ESC11 in mice bearing SK-Mel-187 xenografts after 3 hrs (black bars), 24 hrs (striped bars) 48 hrs (grey bars) and seven days (white bars). Results are presented as percentage of injected dose per gram of tissue. Error bars represent SD (n=4) (D).

Figure 5. Radioimmunotherapy in nude mice bearing subcutaneous FAP-positive SK-MEL-187 tumors: Tumor bearing mice were treated intravenously with 8 MBq (15 µg) ^{177}Lu-labeled antibodies or PBS 5 days after tumor implantation (arrow). **A.** Tumor growth curves showing mean tumor volumes +SD. Curves were plotted until the first tumor per group reached 1000 m^3. B. Kaplan-Meier survival curves of treated and control groups. P-values were obtained with a log rank test. **C.** Ki67 stained and **D.** H&E stained tumor slices on days 0, 3 and 7 after injection of radiolabeled antibodies. Scale bar: 100 µm.

Table 1

	K_DApp on huFAP	**K_DApp on muFAP**
	[nM]	**[nM]**
ESC11 Fab fragment	4.7 ± 1.6	51 ± 11
ESC14 Fab fragment	205 ± 35	251 ± 42
ESC11 IgG1	1.1 ± 0.1	1.8 ± 0.3
ESC14 IgG1	1.1 ± 0.4	2.1± 0.5
vF19 IgG1	4.2 ± 0.6	n.d.

Figure 1

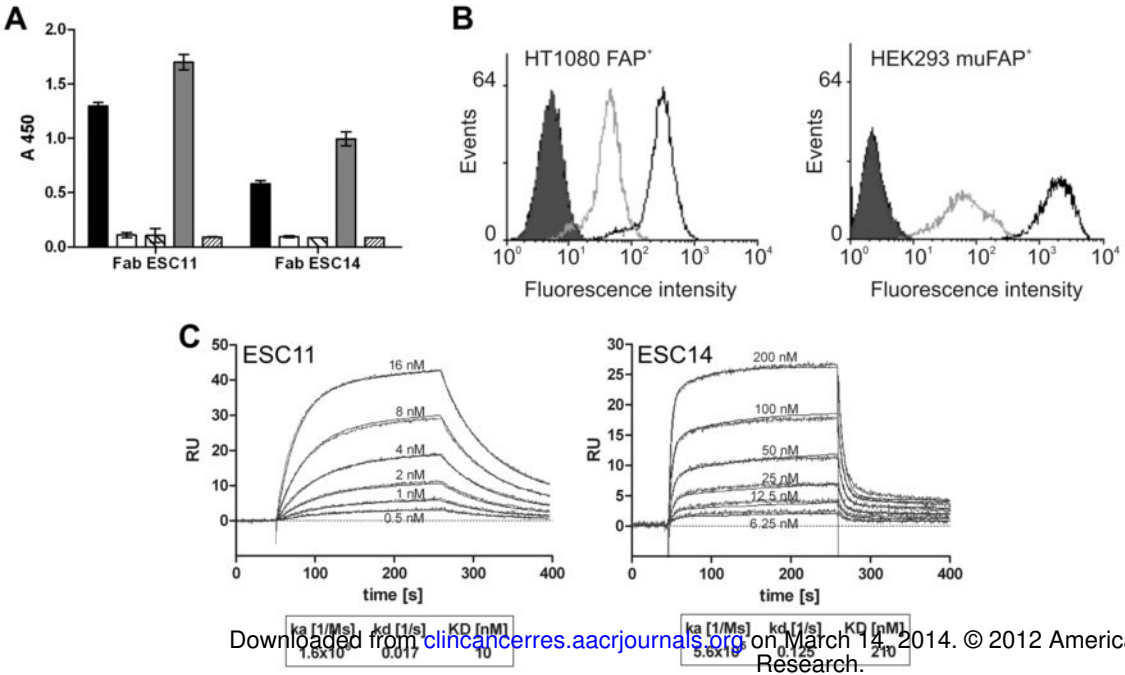

Figure 2

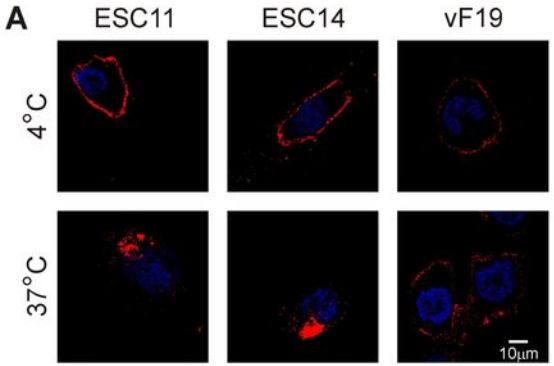

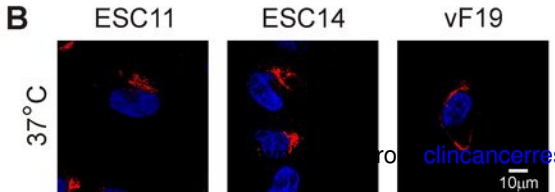

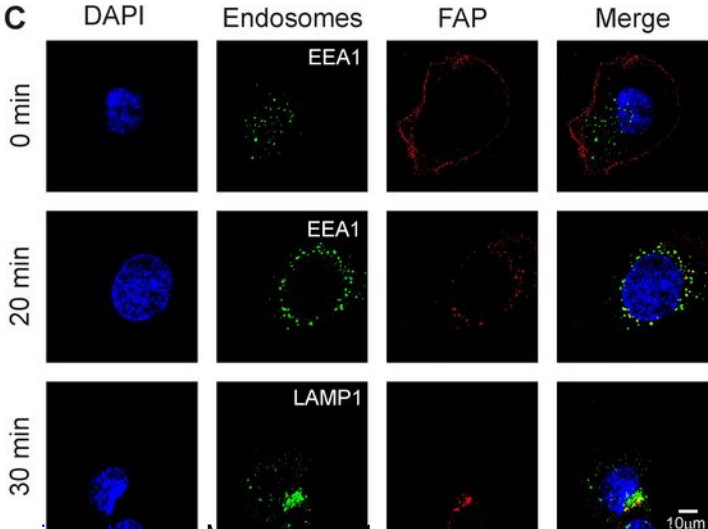

Figure 3

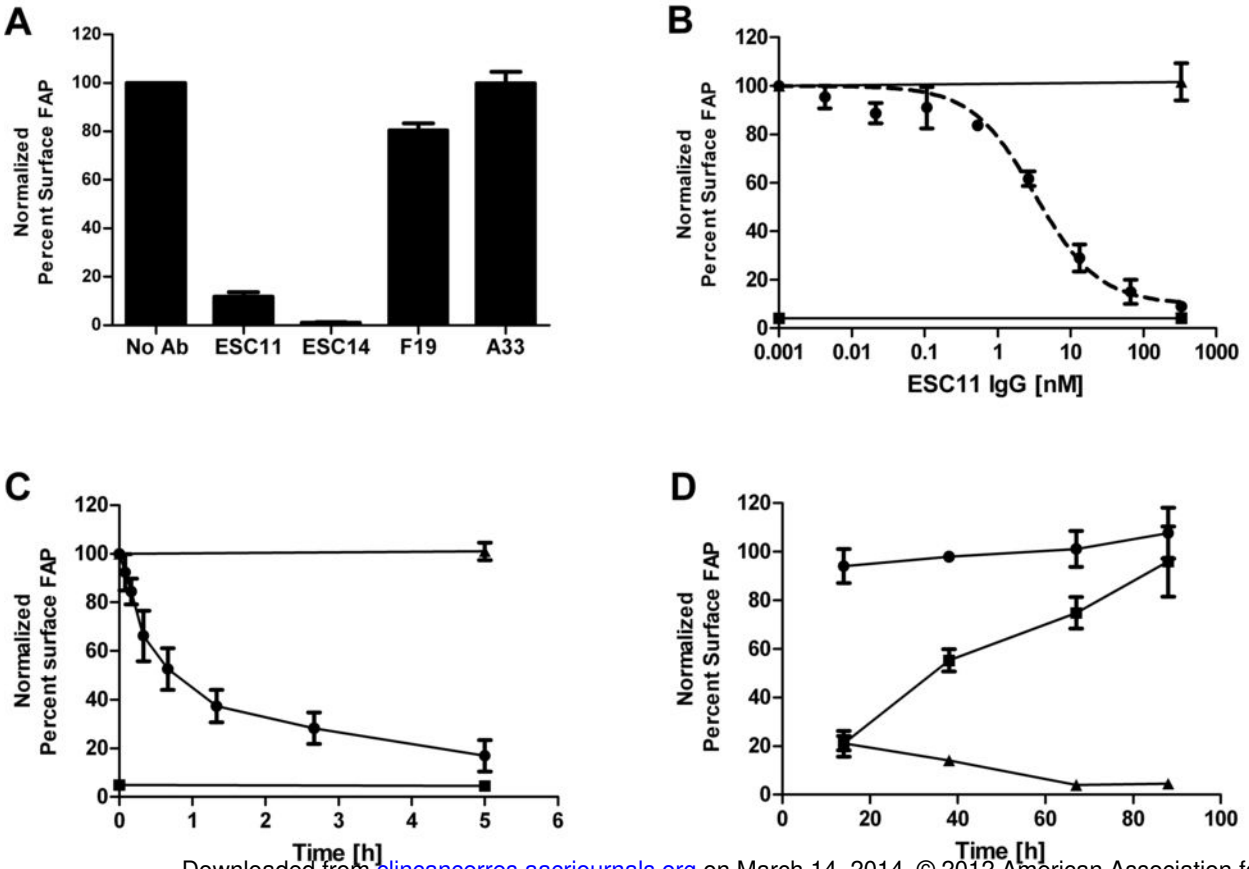

Figure 4

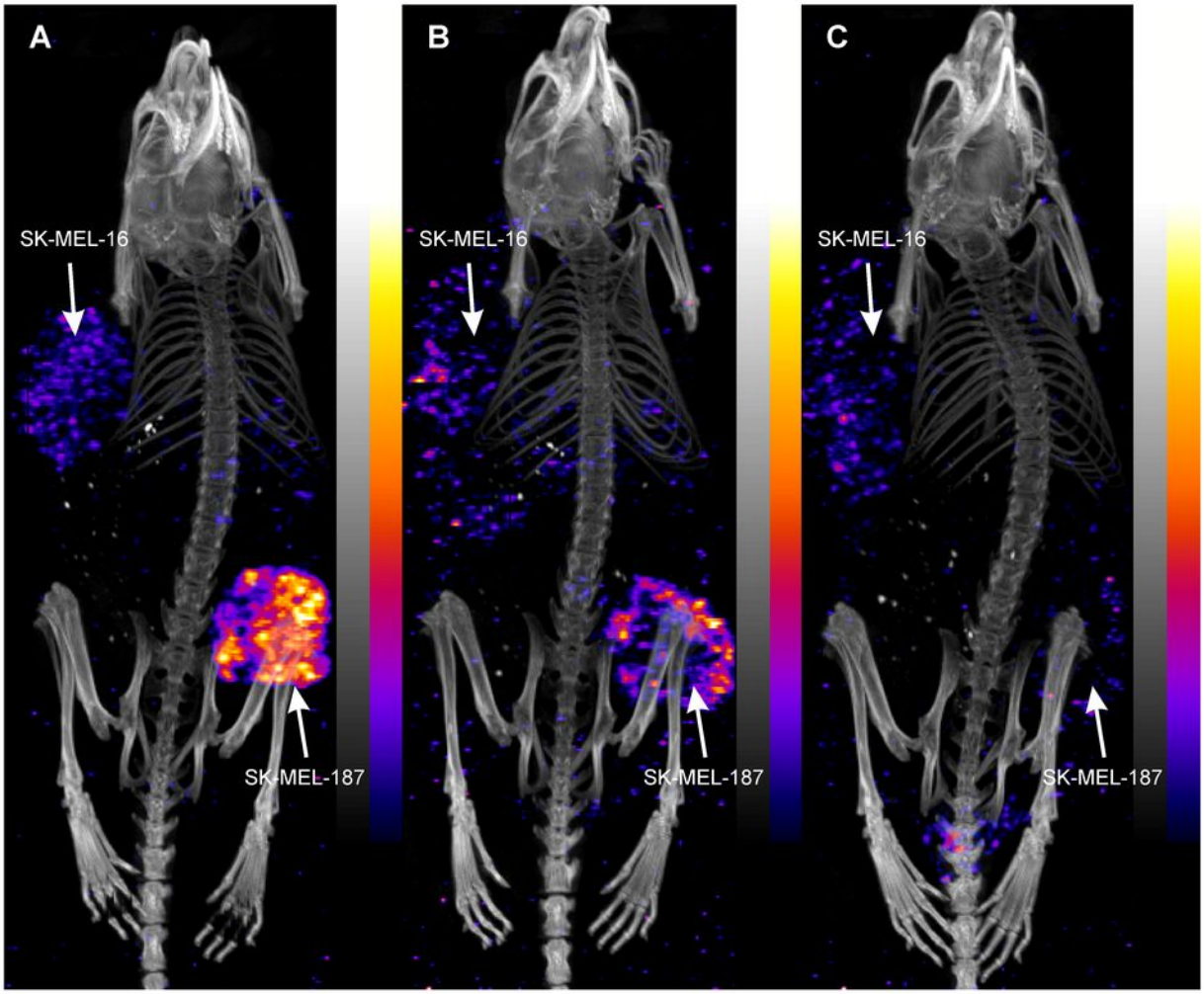

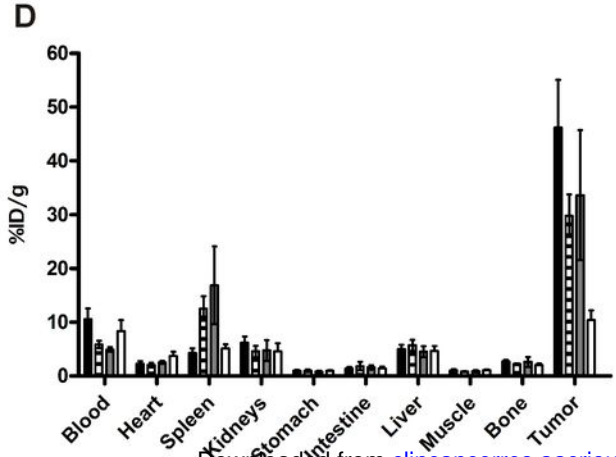

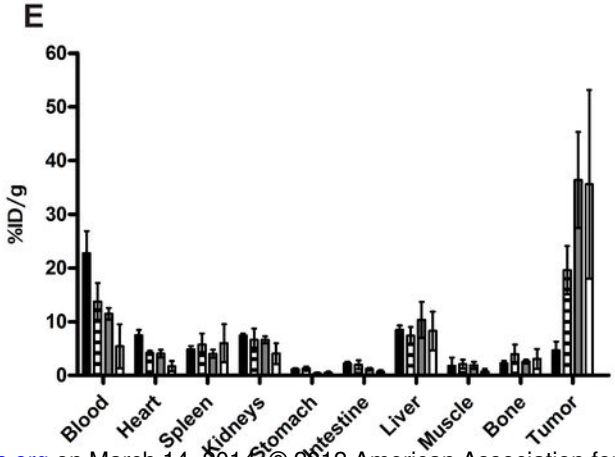

Figure 5